A Novel Optimal Power Management Strategy for Plug-in Hybrid Electric Vehicle with Improved Adaptability to Traffic Conditions

Yuanjian Zhang[1], Chongfeng Wei[2], Yonggang Liu[3], Zheng Chen[4,5*], Zhuoran Hou[6], and Nan Xu[6**]
[1]School of Mechanical and Aerospace Engineering, Queen's University of Belfast, BT9 5AG, Northern Ireland
[2]Department of Mechanical and Construction Engineering, Northumbria University, NE1 8QH, UK
[3]State Key Laboratory of Mechanical Transmissions & School of Automotive Engineering, Chongqing University, Chongqing, 400044, China
[4]Faculty of Transportation Engineering, Kunming University of Science and Technology, Kunming, 650500, China
[5]School of Engineering and Materials Science, Queen Mary University of London, London, E1 4NS, United Kingdom
[6]State Key Laboratory of Automotive Dynamic Simulation and Control, College of Automotive Engineering, Jilin University, Changchun, 130022, China
Email: y.zhang@qub.ac.uk, chongfeng.wei@northumbria.ac.uk, andylyg@umich.edu, chen@kust.edu.cn, houzr20@mails.jlu.edu.cn, nanxu@jlu.edu.cn
Corresponding Author: Zheng Chen (chen@kust.edu.cn) and Nan Xu (nanxu@jlu.edu.cn)

Abstract: Adaptability to various driving conditions (TCs) is one of the essential indicators to assess the optimality of power management strategies (PMSs) of plug-in hybrid electric vehicles (PHEVs). In this study, a novel optimal PMS with the improved adaptability to TCs is proposed for PHEVs to achieve the energy-efficient control in momentary scenarios by virtue of advanced internet of vehicles (IoVs), thus contributing to remarkable promotion in fuel economy of PHEV. Firstly, the optimal control rules in the novel PMS, corresponding to diverse driving conditions, are optimized offline by the chaotic particle swarm optimization with sequential quadratic programming (CPSO-SQP), which can effectively endow the global optimization knowledge into the rule inspired method. Then, an online TC identification (TCI) method is designed by cooperatively exploiting multi-dimensional Gaussian distribution (MGD) and random forest (RF), where the MGD based analysis on the macrocosmic state of traffic contributes to valuable inputs for the RF based TC classification, and additionally the super regression ability of RF further improves the identification accuracy. Finally, the numerical simulation validations showcase that the novel optimal PMS can reasonably and instantly manage the power flow within power sources of PHEV under different TCs, manifesting its anticipated preferable controlling performance.

Key words: Power management strategy (PMS), chaotic particle swarm optimization with sequential quadratic programming (CPSO-SQP), multi-dimensional Gaussian distribution (MGD), random forest (RF), plug-in hybrid electric vehicles (PHEVs).

I. INTRODUCTION

The critical social problems, including energy dilemma and global warming, accelerate the evolution of technologies in all disciplines [1-3]. Plug-in hybrid electric vehicles (PHEVs), as one of extraordinary solutions in

auto industry to solve the mentioned social conflicts, have attained remarkable popularization in recent years [4, 5]. Due to the high-efficiency co-operation scheme between efficient internal combustion engines (ICEs) and power batteries, PHEVs show exceptional abilities in energy reservation and emission reduction [6]. However, the additional energy degrees of freedom, despite huge advantages, make the power management strategies (PMSs) more difficult to manage power flow within different energy sources, especially when facing with different traffic conditions (TCs). To fully excavate the potency of PHEVs in energy saving, PMSs should be more efficient and effective under different traffic conditions (TCs), which is an intractable task waiting to be solved.

A slew of attempts on PMSs (also known as energy management strategies) have been spurred to facilitate power allocation in the powertrain of PHEVs. Existing solutions can be divided into three types: rule based strategies [7, 8], global optimization based strategies [9, 10] and instantaneous based strategies [11, 12]. On the other hand, the substantial progress in artificial intelligence expedites the application of machine learning algorithms in power management of PHEVs and advances substantial improvement in energy saving [13, 14]. However, the raised methods cannot reach the stable game balance among real implementation ability, optimal control effect and computation burden. Rule based strategies, including multi-threshold methods [15] and fuzzy logic algorithms [16], can be instantaneously applied in engineering practice without imposing massive computation burden on on-board hardware; whereas the expert knowledge based design alienates the controlling effect from optimum. Global optimization based methods, such as dynamic programming (DP) [17] and Pontryagin's minimum principle (PMP) [18], declare to achieve remarkable global optimal controlling effect; nonetheless, the burdensome computation discredits their implementation in real time. The instantaneous based strategies, like equivalent consumption minimization strategy (ECMS) [19] and model predictive control (MPC) [5], are eligible in real-time application with the anticipated controlling effect; while the environment-sensible inner parameters in these methods discount the application effect. For example, the equivalent factors (EFs) in ECMS [20], particularly, are highly dependent on appropriate tuning under different driving conditions.

To promote the performance of instantaneous based strategies, adaptive adjustment has been made for tailoring different driving demands/scenarios. Adaptive ECMS (A-ECMS) [21] and stochastic MPC [22] are raised and applied with the improved instantaneous performance. In these adaptive methods, TC identification (TCI) or prediction (TCP) is usually conducted ahead of controlling order determination. These TCI or TCP techniques provide valuable priori knowledge for future driving conditions, and the knowledge can contribute to promotion of the power management effect. Currently, the widely accepted TCI methods are machine learning algorithms, such as

neural network (NN) [23], support vector machine (SVM) [24], and the inputs of these machine learning methods are usually derived from the statistical analysis of traffic state, whereas the simple statistical analysis cannot describe TCs elaborately. Similar with the TCI methods, TCP is usually realized by machine learning methods like NN [25], Markov Chain (MC) [26], etc. These TCP methods can predict the demand based on a large amount of historical training data. Even so, the prediction accuracy will be rapidly deteriorated with the increase of prediction length. Compared with TCP, TCI highlights better application capacities in real time, as it can be periodically performed, rather than completed in each control step. Recently, the flourishing reinforcement learning (RL) and deep RL based methods are progressively emerging in the evolved progress of intelligent decision that eliminate the stickiness between PMSs and environmental information. However, the time-consuming offline preparation of methods, such as Q-leaning [27] and deep Q-learning [28], discredits the real-time implementation potential in current stage.

Although existing machine learning based PMSs have shown progress in improving the adaptability to TCs, their intensive calculation requirement increases the on-line implementation difficulty. Motivated by this, a novel adaptive PMS on the basis of rule based strategy is proposed for a 4-wheel drive (4WD) PHEV with superior promotion in energy saving. In this strategy, a new TCI method is innovatively designed to identify TCs rationally and precisely through random forest (RF). Instead of classifying TCs based on the general statistical results of traffic state, such as average speed and average acceleration, the novel TCI method categorizes the driving conditions according to the characteristic indexes, which are generated through the multi-dimensional Gaussian distribution (MGD) analysis imposed on the shared data from volunteer vehicles on the same route segments. To promote the mediocre controlling performance of rule based PMSs caused by the expert-knowledge dominated design, the chaotic particle swarm optimization (PSO) with sequential quadratic programming (CPSO-SQP) is assigned to optimize control thresholds in the developed PMS under different driving conditions. Meanwhile, the optimal control thresholds are designed in terms of the identified TC for practical implementation. Unlike the existing complex methods whose instant application cannot be easily implemented, the novel developed PMS tries to further advance the potential of the rule-inspired method, intensifying the adaptability to various TCs in optimal control without scarifying the advantage in instant implementation. The meta-heuristic algorithm infuses the supplemental optimal knowledge into expert experience, and the TCI with advanced machine learning methods and IoV framework promotes the environmental adaptiveness. The main contributions added to the literature include:

1) A novel PMS based on the simple rule based algorithm is designed for PHEV by cooperatively coordinating the offline global optimization and online TCI, leading to qualified superior performance in energy saving under

diverse driving scenarios. The proposed novel PMS is an efficient attempt to further excavate the capacity of simple rule based algorithms in instantaneous applications by incorporating the optimal knowledge into the expert experience.

2) The control thresholds in rule based algorithms, corresponding to different driving conditions, are optimized by the CPSO-SQP, which avoids the global optimization caught in local optimum and ensures the optimization effect, compared with standard particle swarm optimization (PSO).
3) The online TCI is attained via the RF based identification algorithm. To refine the accuracy of TCI, the inputs of RF based identification algorithm are carefully designed, including information of the macrocosmic traffic state from the MGD based analysis, which reinforces the identification accuracy via the capability in describing relationships of multi-dimension data.

Aiming to develop the novel PMS for a 4WD PHEV with the prompted performance in time-varying TCs, the remainder of this paper is organized as follows. The studied PHEV and the related model construction are described in Section II. The designed PMS, including the novel TCI method and control threshold optimization algorithm, is detailed in Section III, and the in-depth simulation evaluation in terms of the raised method is conducted in Section IV via comparison studies. The main conclusions are drawn in Section VI.

II. 4WD PHEV AND MODEL CONSTRUCTION

2.1 The Studied 4WD PHEV

The studied 4WD PHEV includes two sets of power units installed on each axle, and the general configuration is shown in Fig. 1 (a). In the front axle, ICE, together with the high-speed generator and motor 1, provides the tractive power. In the rear axle, motor 2 outputs tractive power and recycles braking energy individually. The 4WD PHEV can operate in different modes through the cooperation among ICE, motor and generator, providing better driving power and energy saving potential, compared with two-wheel driven (2WD) PHEVs. In the vehicle, ICE can either drive the vehicle directly with motors in parallel mode, or supply tractive power through driving the generator in serial mode. In serial mode, ICE drives generator to output the required power indirectly. ICE and generator are functioned as an auxiliary power unit (APU) in serial mode. The switch between serial mode and parallel mode is attained by controlling the engagement/disengagement of the clutch between ICE and motor 1. In addition, the 4WD PHEV can operate in pure electric (EV) mode and is driven by motors 1 and 2 together. The detailed parameters of powertrain in the 4WD PHEV are listed in Table 1.

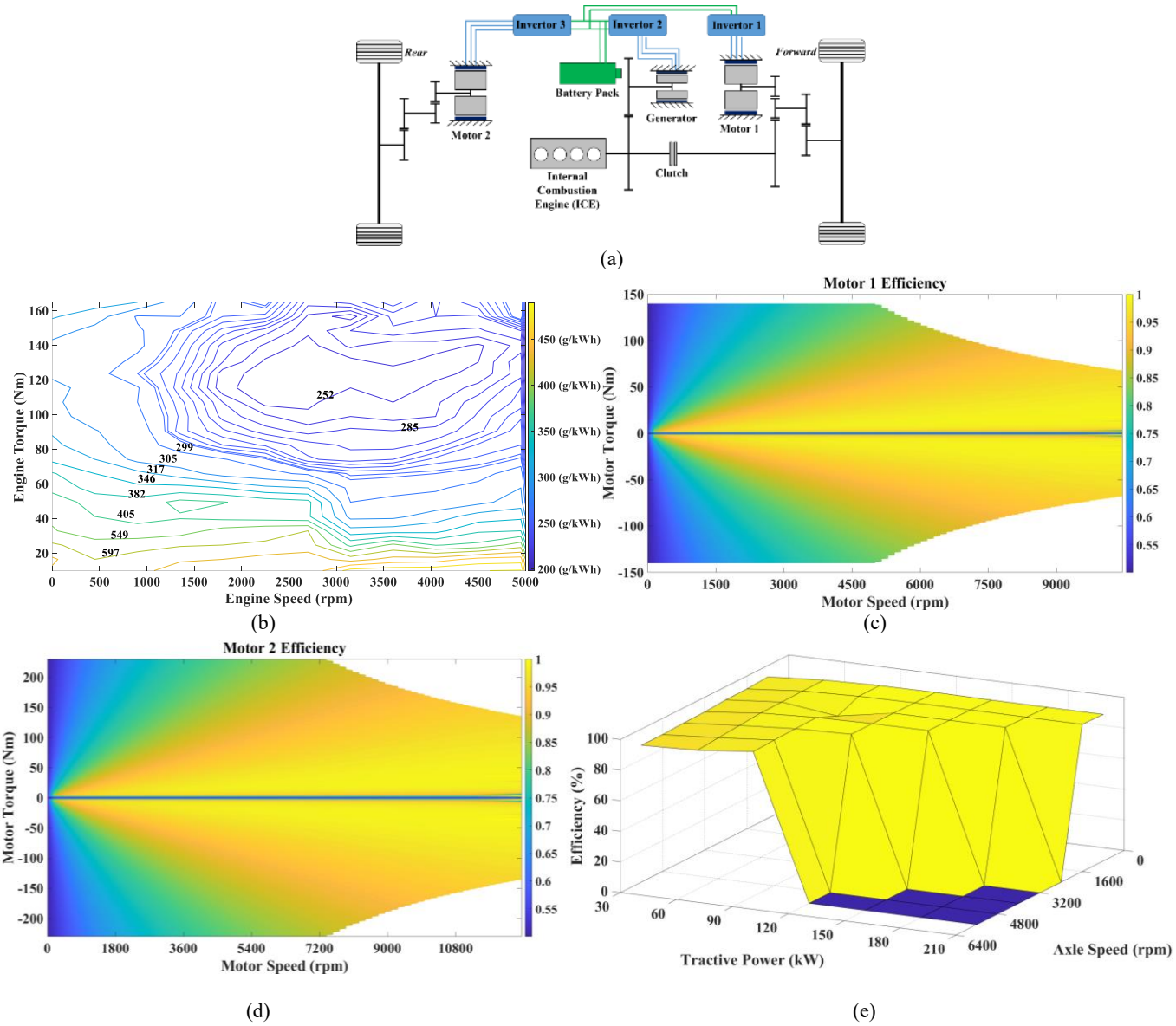

Fig. 1. The details of the 4WD PHEV and model. (a) Schematic of the 4WD PHEV. (b) Efficiency map of ICE. (c) Efficiency map of motor 1. (d) Efficiency of motor 2. (e) Final gear transmission efficiency map.

2.2 4WD PHEV Model Construction

Vehicle models, including backward and forward types, play an essential role in PMS development of PHEVs. The backward models show great convenience in energy estimation, while the forward models are widely adopted in modern vehicle development due to the specific energy transmission direction. In forward models, control units are in charge of translating the driving intentions instructed from drivers and disseminating the corresponding control commands power units. Thus, the forward model is obviously more suitable for developing the adaptive PMS. In this paper, the 4WD PHEV forward model is built in Matlab/Simulink, and there exist four sub-modules: driver module, plant module, controller module and central area network (CAN) module. The driver module concerns driving behaviours and outputs the driving requirement to the controller module, which selects the suitable operation mode and distributes driving power within different power sources. The plant module responds to the given control orders

from the controller module dynamically. The CAN module bridges communication channels among driver, plant and controller module. The mathematic equations of models in terms of each module and component will be described in the next step.

Table 1 Component Parameters in the studied 4WD PHEV

Engine	**Displacement**	**2.0 [L] 16V DOHC**
	Maximum Power	89 [kW] @4500 [rpm]
	Maximum Torque	190 [Nm] @4500 [rpm]
Motor 1	Maximum Power	60 [kW]
	Maximum Torque	137 [Nm]
Motor 2	Maximum Power	60 [kW]
	Maximum Torque	230 [Nm]
Battery	Type	Lithium iron phosphate
	Capacity	16 [kWh]/53.3 [Ah]
	Nominal Voltage	300 [V]
Gear Ratio	Between ICE and final drive	i_{g1}=3.425
	Between motor 1 and final drive	i_{g2}=9.663
	Between motor 2 and final drive	i_{g3}=7.065
	Between ICE and generator	i_{g4}=2.736

A. Driver Model

The driver model describes the driving behaviours and generates the corresponding driving requirement. The input of model is the target velocity derived from the difference between driving cycle data and current simulation velocity, and the output of the model is the degree of acceleration pedal and brake pedal. Normally, the typical proportional-integral-differential (PID) method (simplified to the proportional control in this study) is applied in the driver model, of which the mathematical function can be formulated as:

$$\begin{cases} P_{acc}(t) = K_p(v_{target}(t+1) - v_{real}(t)) \\ P_{brake}(t) = K_p(v_{real}(t) - v_{target}(t+1)) \end{cases} \quad (1)$$

where P_{acc} and P_{brake} denote the expected acceleration and brake pedal degree, v_{target} and v_{real} are the target velocity and simulated velocity, K_p is the scale factor, and t is the time step.

B. ICE Model

Based on the efficiency map acquired through the benchmark test, a static model is adopted to characterize the ICE's nonlinear performance in fuel consumption, as shown in Fig. 1 (b). As such, the instantaneous fuel consumption can be calculated, as:

$$\dot{m}_f(t) = f(T_{out}(t), n_{eng}(t)) \quad (2)$$

where $\dot{m}_f$ is the fuel consumption rate, T_{out} denotes the engine torque, and n_{eng} means the engine speed. Moreover, the engine load L_{eng} can be calculated, as:

$$L_{eng}(t)=\frac{[P_{eng\_re}(t+1)\times 9550]/n_{eng}(t)}{T_{table\_eng(i)\_100\%}} \tag{3}$$

where P_{eng_re} is the required engine power at next time step, and $T_{table\_eng(i)\_100\%}$ denotes the maximum torque corresponding to current engine speed.

C. Motor and Generator Model

The motor and generator in the studied PHEV are permanent magnet synchronous motors (PMSMs). Due to the fast transient response, the dynamic behaviours of electric motor are neglected. Likewise, the static models based on efficiency maps from benchmark test, are employed to describe the power performance of motor and generator, as shown in Fig. 1 (c) and (d). The parameters of generator are the same with motor 1 in this paper. The load of motor and generator can be calculated, as:

$$\begin{cases} L_{mot}(t)=\dfrac{[P_{mot\_re}(t+1)\times 9550]/n_{mot}(t)}{T_{table\_}mot\_100\%} \\ L_{gen}(t)=\dfrac{[P_{gen\_re}(t+1)\times 9550]/n_{gen}(t)}{T_{table\_gen\_100\%}} \end{cases} \tag{4}$$

where L_{mot} and L_{gen} denote the motor and generator load; P_{mot_re} and P_{gen_re} are the required motor power and generator power; n_{mot} and n_{gen} represent the motor speed and generator speed; and $T_{table\_mot\_100\%}$ and $T_{table\_gen\_100\%}$ are the maximum motor torque and generator torque corresponding to the current speed, respectively.

D. Battery Model

The battery pack in the studied PHEV belongs to lithium iron phosphate batteries and is with a nominal capacity of 53.3 Ah in total. The nominal voltage of battery pack is 300V, with 100 cells connected in series. As well known, battery's performance can be influenced by operating temperature and degrades with aging. The designed strategy, however, considers single-step control process every time. Consequently, it is fair to assume there exists limited impact on the performance of vehicle control from temperature and aging degradation in one-step control. As such, the temperature and aging influence are neglected for ease of modelling the battery, and a simple equivalent circuit model is employed to characterize the battery's electrical performance. It consists of an open circuit voltage source and an internal resistor connecting in series topology. By analysing the model of battery, the deviation of SOC can be calculated as:

$$\dot{SOC}(t)=-\frac{V_{oc}(t)-\sqrt{V_{oc}(t)-4R_{\text{int}}(t)P_{batt}(t)}}{2R_{\text{int}}(t)Q_{batt}} \tag{5}$$

where SOC is the battery SOC, V_{oc} is the open circuit voltage of battery, R_{int} is the internal resistance of battery, P_{batt} is the battery power, and Q_{batt} denotes the battery capacity.

E. PMS in Vehicle Model

The addressed PMS in PHEVs, generally, is in charge of operation mode selection and power management. The general control framework is shown in Fig. 2. The control orders from PMS are usually the load rates of components, including throttle values and battery currents calculated according to energy distribution results, and they will be sent to component control units from higher level controller. The logic to control the mode transition in the studied PHEV is designed by a rule based method according to the benchmark test data. The operation mode is commanded to switch by referring to the vehicle speed v, the required tractive power P_{req} and the required tractive torque T_{req}. The thresholds determining the mode transition are illustrated in Fig. 3, in which there exists a rectangular area in both charging depleting and charging sustaining stage. In addition, it is desired to avoid the frequent switch among pure electric, serial and parallel modes, thereby contributing to better driving comfort and fuel economy.

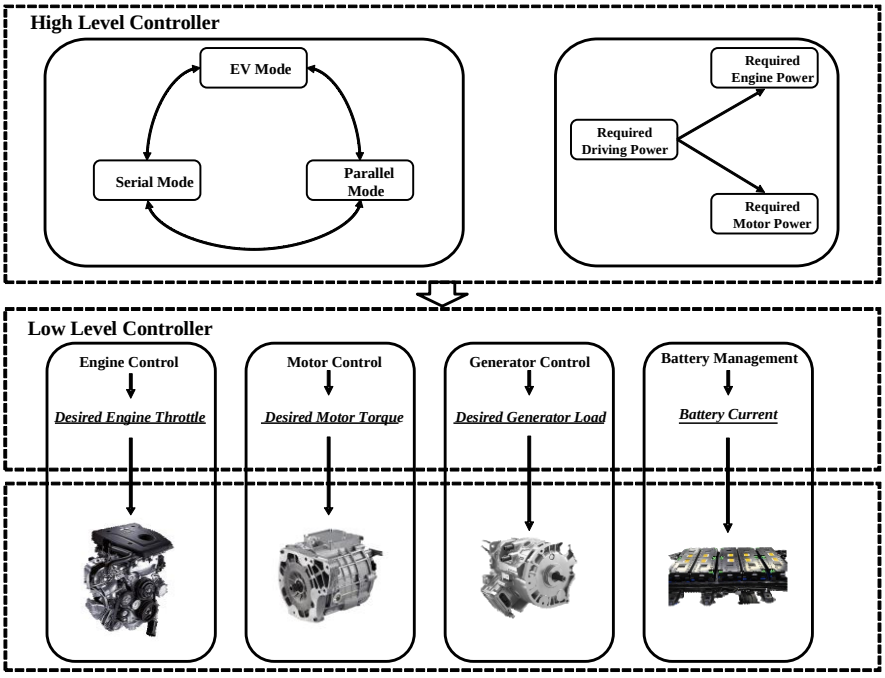

Fig. 2. General control framework in PHEVs.

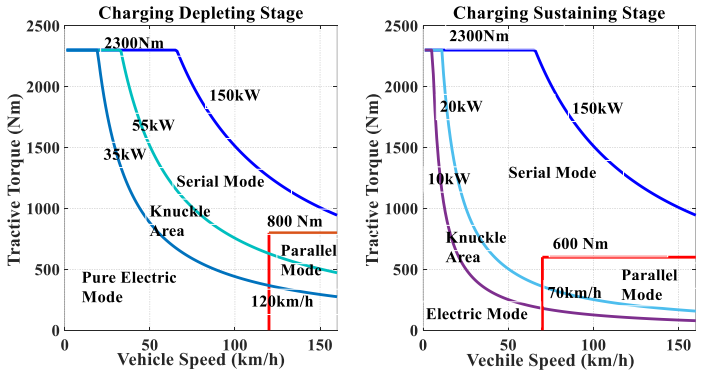

Fig. 3. Mode transition conditions in charging depleting and charge sustaining stage.

In the PMS, the general power management principle is to regulate the engine to operate in the brake-special fuel consumption (BSFC) line by the load-following method. The power management in serial and parallel mode in charging depleting (CD) and charge sustaining stage (CS) can be explained in Tables 2 and 3, respectively.

Table 2 Power management strategy in CD and CS stage under the serial mode

$P_{req} < P_{apu\_opt}$	$P_{apu} = 0$	$P_{batt} = P_{req} \Big/ 2\eta_{mot1}\eta_{tran\_ele1} + P_{req} \Big/ 2\eta_{mot2}\eta_{tran\_ele2}$
$P_{apu\_opt} \le P_{req} < (P_{apu\_opt} + P_{batt\_\max\_CD\_s})$ or $P_{apu\_opt} \le P_{req} < (P_{apu\_opt} + P_{batt\_\max\_CS\_s})$	$P_{apu} = P_{apu\_opt}$	$P_{batt} = (P_{req} - P_{apu\_opt}\eta_{mot1}\eta_{tran\_ele\_apu}) \Big/ 2\eta_{mot1}\eta_{tran\_ele1} + (P_{req} - P_{apu\_opt}\eta_{mot1}\eta_{tran\_ele\_apu}) \Big/ 2\eta_{mot2}\eta_{tran\_ele2}$
$(P_{apu\_opt} + P_{batt\_max\_CD\_s}) < P_{req}$ or $(P_{apu\_opt} + P_{batt\_max\_CS\_s}) < P_{req}$	$P_{apu} = P_{apu\_max}$	$P_{batt} = (P_{req} - P_{apu\_max}\eta_{mot1}\eta_{tran\_ele\_apu}) \Big/ 2\eta_{mot1}\eta_{tran\_ele1} + (P_{req} - P_{apu\_max}\eta_{mot1}\eta_{tran\_ele\_apu}) \Big/ 2\eta_{mot2}\eta_{tran\_ele2}$

Note that P_{apu} expresses the APU power, P_{apu_opt} denotes the power corresponding to the optimal operation points of APU, P_{apu_max} represents the maximum power corresponding to the specific speed of APU. $P_{batt\_max\_CD\_s}$ and $P_{batt\_max\_CS\_s}$ mean the maximum power limit of battery in the charge depletion and charge sustaining stage when the vehicle is under the serial mode. P_{req} denotes the required driving power; $\eta_{tran\_ele\_apu}$, η_{tran_ele1} and η_{tran_ele2} denote the transmission efficiency of the electric path between APU and motor 1, between battery and motor1, and between battery and motor 2, respectively; and η_{mot1} and η_{mot2} is the efficiency of motors 1 and 2.

Table 3 Power management strategy in CD and CS stage under the parallel mode

$P_{req} < P_{eng\_opt}$	$P_{eng} = 0$	$P_{batt} = P_{req} \Big/ 2\eta_{mot1}\eta_{tran\_ele1} + P_{req} \Big/ 2\eta_{mot2}\eta_{tran\_ele2}$
$P_{eng\_opt} \le P_{req} < (P_{eng\_opt} + P_{batt\_\max\_CD\_p})$ or $P_{eng\_opt} \le P_{req} < (P_{eng\_opt} + P_{batt\_\max\_CS\_p})$	$P_{eng} = P_{eng\_opt}$	$P_{batt} = (P_{req} - P_{eng\_opt}\eta_{tran\_fuel}) \Big/ 2\eta_{mot1}\eta_{tran\_ele1} + (P_{req} - P_{eng\_opt}\eta_{tran\_fuel}) \Big/ 2\eta_{mot2}\eta_{tran\_ele2}$
$(P_{eng\_opt} + P_{batt\_max\_CD\_p}) < P_{req}$ or $(P_{eng\_opt} + P_{batt\_max\_CS\_p}) < P_{req}$	$P_{eng} = P_{eng\_max}$	$P_{batt} = (P_{req} - P_{eng\_max}\eta_{tran\_fuel}) \Big/ 2\eta_{mot1}\eta_{tran\_ele1} + (P_{req} - P_{eng\_max}\eta_{tran\_fuel}) \Big/ 2\eta_{mot2}\eta_{tran\_ele2}$

Note that P_{eng} is the engine power, P_{eng_opt} denotes the power corresponding to the optimal operation points of ICE, P_{eng_max} represents the maximum power corresponding to the specific speed of ICE. η_{tran_fuel} denote the transmission efficiency of fuel path.

In addition, the transmission efficiencies of fuel and electric paths are calculated by the multipliers of the efficiency of gear i_{g1}, i_{g2}, i_{g3} and i_{g4} with final gear efficiency. The efficiency of i_{g1}, i_{g2}, i_{g3} and i_{g4} is all set to 0.95 in this study. The final gear efficiencies can be attained via the interpolation based on the efficiency map according to the current axle speed and required tractive powers, as shown in Fig. 1 (e). The target of PMS addressed in this paper is applied to optimally assign the operation modes and distribute the energy ratios within the powertrain system in real-time, and the solution searching in the designed strategy is based on the efficiency maps of ICE and motors, which have considered the impact from thermal dynamics. The transient thermal behaviors of ICE and motors,

consequently, are not considered separately in the PMS development. Additionally, it is assumed that battery temperature will not increase significantly in each control step.

In the next step, based on the detailed modelling of powertrain components, the proposed novel PMS will be elaborated and discussed.

III. Development of the Novel PMS

The developed PMS is qualified with the extraordinary adaptability to environment variation based on the accurate TCI. Even though the principle underlining the novel strategy is essentially the simple rule based control logic, the offline control threshold optimization can translate the valuable knowledge of optimization to expert experience. Fig. 4 illustrates the general control process of the raised method. The historical traffic data is gathered for the offline K-means based clustering operations [29], thereby generating three different driving conditions: slow-moving, medium-speed drag-free and high-speed transit, corresponding to the driving in city downtown, urban and highway, respectively. Given the specifically derived driving cycle belonging to certain TC, the CPSO-SQP optimizes the controlling thresholds existing in the rule-based strategy and generates the optimal parameter set for real-time implementation. The collected historical traffic data are analysed by the MGD, thus forming specific data to train the RF to realize the instantaneous TCI. The MGD based traffic flow analysis describes the traffic state from multiple perspectives, rather than the simply statistical quantity in existing methods, leading to more accurate TCI. In actual applications, instantaneous traffic data will be processed by the MGD online for the RF based TCI. According to the classified TC, the specific control thresholds are assigned to hybrid powertrains to achieve efficient mode selection and energy distribution. In the next step, the methods to classify different TCs based on specific data processed by the MGD and CPSO-SQP based offline parameter optimization will be introduced in detail.

3.1 MGD and RF Based TCI

As discussed before, the identified TCs are critical to prompt the power management performance of PHEVs. Existing methods classify TCs by statistically analysing the numerical variables related with traffic status. The numerical variables including the average velocity, average acceleration and percentage of different speed ranges, are usually adopted to quantify the traffic status include. Despite the validated performance under certain conditions, the developed TCI methods shows some obvious disadvantages:

1) Simple numerical variables seldom present inner connections among each other and thus cannot describe TCs accurately and minutely.

2) Existing TCI methods, based on the numerical variables, impress large number of inputs into TC identification algorithms such as NN and SVM, thereby complicating the training process and hindering implementation in real time.

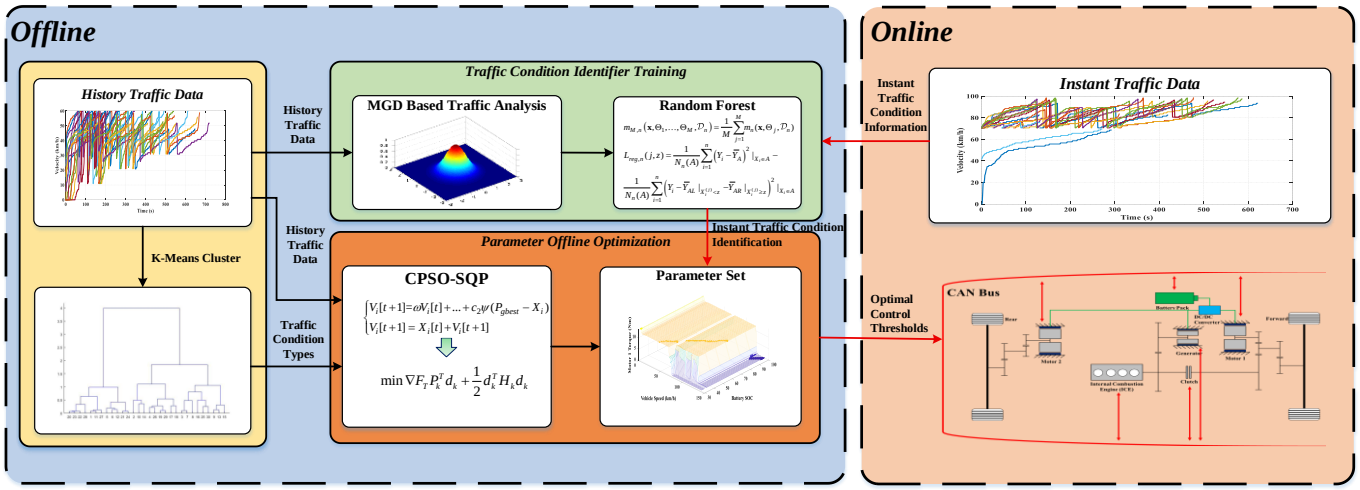

Fig. 4. Control process of the novel PMS.

To improve the accuracy of TCI in real time, a novel TCI method is proposed in this study. Instead of categorizing TCs by analysing the given numerical variables related to traffic status, the RF based TC identification algorithm classifies them with the inputs from the MGD based analysis in terms of the shared traffic information. The traffic flow analysis through MGD can sufficiently reveal traffic state by investigating the interaction among multiple factors. Benefiting from the internet of vehicles (IoVs), vehicle status, including velocity, acceleration and distance headway to forward vehicle, can be easily shared within vehicles on certain route segment via vehicle to vehicle (V2V) communication. Besides, general traffic status like the number of vehicles on the route segment can be disseminated to each vehicle via vehicle to infrastructure (V2I) communication. It is assumed that the V2V and V2I adopt the millimeter-wave (mmWave) communication thanks to its ultra-wide band [30]. Meanwhile, to reduce the hardware complexity and energy consumption, the base station (BS) and vehicle are equipped with single radio frequency chain [30].

The execution process of the raised TCI method is illustrated in Fig. 5. Accordingly, the shared traffic information is analysed by the MGD to generate small scale of inputs for te RF based TC identification algorithm, which, installed in on-board vehicle control unit (VCU), identifies the TC for next route segment before vehicle moves in. To guarantee the controlling effect, TCs in next route segment are classified every 20 s, and the total travel time in next segment can be calculated by the method in [1]. The traffic information of next route segment for TCI is instantaneously shared to the target vehicle via the V2V and V2I communication. The input of RF based identification algorithm consists of the number of vehicles on the next route segment, average value and variance of velocities,

acceleration and distance headway on next route segment in three-dimension (3D)-MGD, value of covariance matrix of 3D-MGD on velocity, acceleration and distance headway on next route segment, and probability density of vehicle idle in 3D-MGD. Compared with TCI with 15 to 25 inputs in previous methods [31, 32], the raised method only requires 9 variables for the RF based classification, thereby reducing the scale of identification algorithm. The inputs are chosen after comprehensively considering the interaction between vehicle behaviours and traffic status. The outputs of RF are three classified TCs, including slow-moving, medium-speed drag-free and high-speed transit. The 3D-MGD and RF in the TCI will be introduced in the next step.

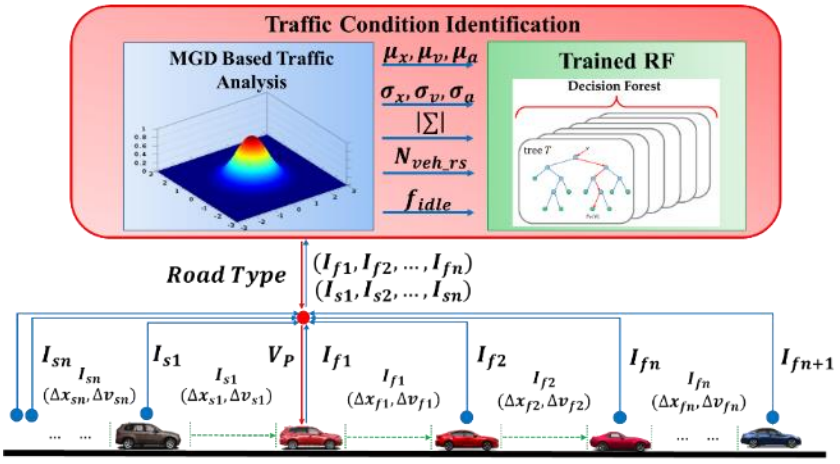

Fig. 5. Illustration on novel TCI method.

A. Traffic Flow Analysis by 3D-MGD

The 3D-MGD is theoretically derived from the basic one dimension (1D)-Gaussian distribution (GD) [33]. For three independent variables $\bar{x} = (x_1, x_2, x_3)$, these independent variables should satisfy:

$$f(x_1, x_2, x_3) = f(x_1) f(x_2) f(x_3) \tag{6}$$

The averages and variances of the independent variables can be expressed as:

$$\begin{cases} \bar{u} = (u_1, u_2, u_3) \\ \bar{\sigma} = (\sigma_1, \sigma_2, \sigma_3) \end{cases} \tag{7}$$

Based on the general description of 1D-GD, equation (6) can be reformulated as:

$$f(\bar{x}) = \frac{1}{(2\pi)^3 / 2(\sigma_1^2 \sigma_2^2 \sigma_3^2)^{1/2}} \exp\left(-\frac{1}{2} \left[\left(\frac{x_1 - u_1}{\sigma_1} \right)^2 + \left(\frac{x_2 - u_2}{\sigma_2} \right)^2 + \left(\frac{x_3 - u_3}{\sigma_3} \right)^2 \right] \right) \tag{8}$$

For the 3D vector, the covariance matrix can be expressed as:

$$\Sigma = \begin{bmatrix} \sigma_1^2 & 0 & 0 \\ 0 & \sigma_2^2 & 0 \\ 0 & 0 & \sigma_3^2 \end{bmatrix} \tag{9}$$

Accordingly, the value of the covariance matrix and inverse covariance matrix can be respectively expressed as:

$$|\Sigma| = \sigma_1^2 \sigma_2^2 \sigma_3^2 \tag{10}$$

$$\Sigma^{-1} = \frac{1}{\sigma_1^2 \sigma_2^2 \sigma_3^2} \begin{bmatrix} \sigma_3^2 & 0 & 0 \\ 0 & \sigma_2^2 & 0 \\ 0 & 0 & \sigma_1^2 \end{bmatrix} \tag{11}$$

By applying (10) and (11) into (8), the 3D-MGD can be formulated, as:

$$N(\bar{x}|\bar{u},\Sigma) = \frac{1}{(2\pi)^{3/2}} \frac{1}{|\Sigma|^{1/2}} \exp\left[-\frac{1}{2} (\bar{x} - \bar{u})^T \Sigma^{-1} (\bar{x} - \bar{u}) \right] \tag{12}$$

In the 3D-MGD based traffic flow analysis, the dependent variables can be described, as:

$$\begin{cases} \bar{x} = (v, a, \Delta x) \\ \bar{u} = (u(v), u(a), u(\Delta x)) \\ \bar{\sigma} = (\sigma(v), \sigma(a), \sigma(\Delta x)) \end{cases} \tag{13}$$

where v, a and Δx respectively means the vehicle velocity, acceleration, and distance headway. The probability density of idle state in 3D-MGD can be acquired by (12) through setting velocity and acceleration to zero, and the value of covariance matrix in 3D-MGD can be calculated by (10). The methods to calculate average and variance of velocity, acceleration, and distance headway in 3D-MGD are the same with that in 1D-GD [33]. In addition, the number of vehicles on the next route segment is counted in cloud sever and shared to the target vehicle timely.

B. TC Identification Algorithm by RF

In the classification problem by RF [34], the supervised classification is realized by the basic binary classification in decision tree. The observed input vector is $\mathbf{X} \in \mathcal{X} \subset c^p$, and the guessed output $\mathbf{Y}$ takes the value in (0,1). Given the raining sample $\mathcal{D}_n = ((X_1, Y_1), \ldots, (X_n, Y_n))$, the classification rule m_n is applied to train the RF. The classification rule is a Borel measurable function of $\mathbf{X}$ and $\mathcal{D}_n$ [35]. Then, RF conducts the classification through a majority vote among the decision trees, as:

$$m_{M,n}(\mathrm{x}; \Theta_1, ..., \Theta_M, \Theta_n) = \begin{cases} 1 & if \ \frac{1}{M} \sum_{j=1}^{M} m_n(\mathrm{x}; \Theta_M, \Theta_n) > \frac{1}{2} \\ 0 & otherwise \end{cases} \tag{14}$$

where $\Theta_1, \ldots, \Theta_M$ are random variables with the same distribution with $\mathcal{D}_n$. By supposing that a leaf is on behalf of region A, the tree classifier can be simplified as:

$$m_{M,n}(\mathrm{x};\Theta_1,...,\Theta_M,\Theta_n)=\begin{cases}1 & if \sum_{i\in D_n^*(\Theta_j)}\prod_{X_i\in A,Y_i\in 1} > \sum_{i\in D_n^*(\Theta_j)} > \prod_{X_i\in A,Y_i\in 0} \\ 0 & otherwise\end{cases} \tag{15}$$

where $D_n^*(\Theta_j)$ denotes the data points selected in the resampling step. In this paper, the classification and regression tree (CART) [35] is employed in the RF algorithm. For any $(j,\mathrm{z})\in\mathcal{C}_A$, the CART-split criterion can be formulated, as [35]:

$$L_{class,n}(j,z)=p_{0,n}(A)p_{1,n}(A)-\frac{N_n(A_L)}{N_n(A)}p_{0,n}(A_L)p_{1,n}(A_L)-\frac{N_n(A_R)}{N_n(A)}p_{0,n}(A_R)p_{1,n}(A_R) \tag{16}$$

where $\mathcal{C}_A$ is the set of all possible cut, $A_L=\{x\in A: x^{(j)}<z\}$, $A_R=\{x\in A: x^{(j)}\geq z\}$, and $\bar{Y}_A$ (resp., $\bar{Y}_{AL},\bar{Y}_{AR}$) means the average value of Y_i. For each cell A, $p_{0,n}(A)$ is the empirical probability. The pseudo code of RF algorithm is provided in Table 4, where $nodesize\in\{1,\ldots,a_n\}$ is the number of examples in each cell, and $mtry\in\{1,\ldots,p\}$ is the number of possible directions for splitting at each leaf node.

Table 4 The pseudo code of RF algorithm

```
for j = 1,...,M do
  Pick up a_n points in D_n
  Set P = (X)
  Set P_final = ∅
  while P ≠ ∅ do
    Let A be the first element of P
    if A contains less than nodesize points or if X_i ∈ A are equal then
      Remove the cell A from P
      P_final ← Concatenate ( P_final, A)
    else
      Pick up a subset M_try ⊂ {1,..., p} or cardinality mtry
      Choose the most suitable spilt in A by CART-split criterion
      Cut the cell A according to the split. Name A_L and A_R for the two split cells.
      Remove the cell A from the list P
      P ← Concatenate(P, A_L, A_R)
    end
  end
  Compute the estimation value m_n(x, Θ_j, D_n) at x
end
```

3.2 CPSO-SQP Based Control Threshold Optimization

A. General Parameter Optimization by PSO

PSO is one of meta-heuristic algorithms belonging to swarm intelligence and can globally search optimal results [36]. By imitating behaviours of bird flocks, PSO solves optimization problems based on the defined particles. During the optimization process, particles for candidate solutions flow through the search space along the specified direction that is planned according to the best performance of individual particle and swarm [37]. The particles are updated in

each population by learning the cooperation and differentiation among particles. Notably, the particle flow direction should be carefully programmed to avoid the preferred solutions from being trapped into local neighbourhood. Each particle represents a solution of the optimization problem in a D-dimensional space [36]. The position of *i*th particle can be defined as:

$$x_i = [x_{i1}, x_{i2}, ..., x_{iD}] \tag{17}$$

In each population, each particle can be expressed as:

$$X = \{x_1, x_2, ..., x_n\} \tag{18}$$

During searching the optimal solution, each particle updates its position based on its current position and the flowing speed. The position updating manner can be described as:

$$x_i[t+1] = x_i[t] + v_i[t+1] \tag{19}$$

where t is the iteration number, and v_i is the particle flowing velocity. The particle flowing velocity can be calculated, as:

$$v_i[t+1] = \omega v_i[t] + c_1\varphi(P_{besti} - x_i) + c_2\psi(P_{gbest} - x_i) \tag{20}$$

where P_{besti} means the best position of particle i, P_{gbest} is the optimal position among particles, φ and ψ are the uniformly distributed random variables, c_1 and c_2 denote the acceleration coefficients, and φ is the inertial weight. Through the designed velocity, the particles can flow across the searching space efficiently. In the right side of (20), the first term tracks the previous flow direction with a certain weight, preventing searching the deflected direction; the second term studies the tendencies of the personally optimal positions; and the third term identifies the manners that particles move toward the best position. Given the nature of the searching process, local optimality, rather than global one, may be identified with the inappropriately assigned parameters, thus reducing the efficiency of the approach. To assure the effect of parameter optimization, some improvement on PSO deserves to be made.

B. Improved Parameter Optimization by CPSO-SQP

To enhance the performance of PSO by avoiding the solution process in PSO from being trapped in local optimality, the chaotic PSO with sequential quadratic programming (CPSO-SQP), as a two-phased iterative strategy, is advanced. In CSPO-SQP, CLS is applied to reinforce the local oriented optimization, while the SQP is exploited to tune the search results for global optimality [38]. The pseudo code of the CPSO-SQP is provided in Table 5. The CLS is implemented based on the Tent equation [38], as:

$$cx_i^{(k+1)} = \begin{cases} 2cx_i^{(k)}, 0 < cx_i^{(k)} \le 0.5 \\ 2(1-2cx_i^{(k)}), 0.5 < cx_i^{(k)} < 1 \end{cases} \tag{21}$$

where cx_i is the i th chaotic variable, and k denotes the iteration number. The process of CLS can be described as:

1. Initialize $k=0$, and convert the $x_i^{(k)}, i=1,2,\ldots,n$ within $(x_{min,i}, x_{max,i})$ to chaotic variable $cx_i^{(k)}$ in (0,1) by:

$$cx_i^{(k)} = \frac{x_i^k - x_{min,i}}{x_{max,i} - x_{min,i}} \tag{22}$$

2. Calculate $cx_i^{(k+1)}$ for next iteration by (21).

3. Convert $cx_i^{(k+1)}$ to $x_i^{(k+1)}$ by:

$$x_i^{(k+1)} = x_{min,i} + cx_i^{(k+1)}(x_{max,i} - x_{min,i}) \tag{23}$$

4. Evaluate the new solutions with $x_i^{(k+1)}, i=1,2,\ldots,n$,

5. If the new solution is better than $X^{(0)} = [X_1^{(0)}, X_2^{(0)}, \ldots, X_n^{(0)}]$ or iteration limit, output the new solution, or return to step 2.

Table 5 The pseudo code of CPSO-SQP

1	**for** i=1 to *N* **do**
2	parameter initialization
3	**end**
4	**for** n=1 to iteration limit **do**
5	**for** i=1 to *N* **do**
6	$\begin{cases} V_i[t+1] = \omega V_i[t] + c_1\varphi(P_{besti} - X_i) + c_2\psi(P_{gbest} - X_i) \\ V_i[t+1] = X_i[t] + V_i[t+1] \end{cases}$
7	**do** *CLS*
8	**end**
9	**if** $P_{besti} < P_{best(i-1)}$ **then**
10	solve the optimization problem by SQP with start point of P_{besti}
11	**end**
12	**end**

The SQP has been verified effective to find accurate solutions for nonlinear control problems [39]. For SQP, optimal solutions can be obtained by the iterative process. In each iteration, the quadratic programming (QP) problem is solved to indicate the searching direction [40]. Based on the obtained searching direction, the control variables are updated accordingly. The QP problem can be described as:

$$\min \frac{1}{2} d_k^T H_k d_k + \nabla f(x_k)^T d_k \tag{24}$$

subject to:

$$\begin{cases} [\nabla g(x_k)]^T d_k + g_i(x_k) = 0 & i = 1,\ldots,n \\ [\nabla g(x_k)]^T d_k + g_i(x_k) \le 0 & i = n+1,\ldots,m \end{cases} \tag{25}$$

where H_k denotes the Hessian matrix of the Lagrangian function, d_k means the search direction foundation at iteration k, $f(x)$ is the evaluation function in each iteration, $g(x)$ is the constraints on the optimization problem, n is the number of the equality constraints, and m is the number of the constraints. The Hessian matrix of the Lagrangian function can be constructed, as:

$$L(x,\lambda) = f(x) + \lambda^T g_i(x) \tag{26}$$

In the SQP based solution, there are three main steps to proceed: updating the Hessian of the Lagrangian function, solving the QP and calculating the Lagrangian merit function. In the first step, the Hessian of Lagrangian function is updated by the BFGS quasi-Newton method [41], as:

$$B_{k+1} = B_k + \frac{q_k q_k^T}{q_k^T s_k} - \frac{(B_k s_k)(B_k s_k)^T}{s_k^T B_k s_k} \tag{27}$$

where

$$\begin{cases} s_k = x_{k+1} - x_k \\ q_k = \nabla f(x_{k+1}) + \sum_{i=1}^{m} \lambda_i \nabla g_i(x_{k+1}) - \nabla f(x_k) - \sum_{i=1}^{m} \lambda_i \nabla g_i(x_k) \end{cases} \tag{28}$$

In (28), λ denotes the estimation of the Lagrangian multiplier, and H_k is approximately estimated by B_k. At each iteration, the QP problem is solved by (24) to generate the searching direction d_k. In the third step of SQP, the manner to update solution can be expressed, as:

$$x_{k+1} = x_k + a_k d_k \tag{29}$$

where a_k denotes the step length that mainly accounts for adjusting the decrease search of the augmented Lagrangian function, as:

$$L = f(x) - \sum_{i=1}^{m} \lambda_i (g_i(x) - s_i) + \frac{1}{2} \sum_{i=1}^{m} \rho_i (g_i(x) - s_i)^2 \tag{30}$$

where s is the non-negative slack variable, and ρ denotes the penalty parameter. In the control threshold optimization by the CPSO-SQP, the updated particles are the control thresholds in PMS. The optimized control thresholds include the parameters of strategy accounting for mode transition and battery power limits in different modes. The evaluation function $f(x)$ in each iteration can be written as:

$$f(x) = \sum_{t=1}^{N} \left(\dot{m}_f(X) + \omega_t \frac{P_{batt}(X)}{Q_{lhv}} \right) \tag{31}$$

where $\dot{m}_f$ is the instant fuel consumption after determining the optimized control thresholds X on the specified route segment, P_{batt} is the battery power, Q_{lhv} is the fuel low heat value, ω_t denotes the weighting on energy consumption, and t is the time step. The control thresholds determine the mode transition and battery power limits in different operation modes for the PHEV. The constraints on the optimization problem can be summarized, as:

$$\begin{cases} SOC_{\min} \le SOC \le SOC_{\max} \\ P_{batt\_\min} \le P_{batt} \le P_{batt\_\max} \\ T_{eng\_\min} \le T_{eng} \le T_{eng\_\max} \\ T_{mot\_1\_\min} \le T_{mot1} \le T_{mot\_1\_\max} \\ T_{mot\_2\_\min} \le T_{mot2} \le T_{mot\_2\_\max} \\ T_{gen\_\min} \le T_{gen} \le T_{gen\_\max} \\ \omega_{eng\_\min} \le \omega_{eng} \le \omega_{eng\_\max} \\ \omega_{mot\_1\_\min} \le \omega_{mot\_1} \le \omega_{mot\_1\_\max} \\ \omega_{mot\_2\_\min} \le \omega_{mot\_2} \le \omega_{mot\_2\_\max} \\ \omega_{gen\_\min} \le \omega_{gen} \le \omega_{gen\_\max} \end{cases} \tag{32}$$

where the superscripts min and max denote the minimum and maximum value of each variable, respectively. T_{eng}, T_{mot_1}, T_{mot_2} and T_{gen} represent the torque of ICE, motor 1, motor 2 and generator; and ω_{eng}, ω_{mot_1}, ω_{mot_2} and ω_{gen} denote the speed of the ICE, motor 1, motor 2 and generator, respectively. The control thresholds in the designed strategy are optimized offline by the CPSO-SQP on the specific driving cycles. The driving cycles for offline optimization, corresponding to the three TCs, are derived from the historical traffic data. The extracted driving cycles with the same length are obtained by the method in [42]. When the vehicle moves in new route segment, the on-board VCU starts to identify TC of next route segment and assign the corresponding control thresholds subsequently. The vehicle judges the geographic position by referring to the instant GPS coordinates and shared map data.

In the next step, the simulations and detailed comparisons are conducted to validate the feasibility of the proposed algorithm.

IV. Simulation Validation

In this section, simulations are performed to validate the capability of proposed PMS in instant energy management of PHEVs. In the assessment, the effectiveness of novel TCI method and role of the proposed PMS in energy saving are comprehensively assessed through the comparison study, where Original CS means the rule based PMS derived from the benchmark test, NCS with NTCI represents the proposes adaptive PMS. The simulation is performed in the Matlab/Simulink- IPG CarMaker co-simulation platform, in which the IPG CarMaker offers

scenario simulation, and the PMS simulation is conducted in Matlab/Simulink. The connection between PMS and scenario simulation is realized via the interface in IPG Carmaker. The vehicle instant state values obtained in IPG Carmaker, including the velocity, acceleration and time headway of vehicles on route segment, are sent to PMS in Matlab/Simulink through the interface, thereby assisting in accomplishing TCI and power management. Note that all the simulation were conducted on a workstation with an i7-8700 processor and 16 gigabytes memory.

4.1 Assessment on the Effectiveness of the Novel TCI Method

The identification accuracy of TCI method is critical to the proposed adaptive PMS. Therefore, it is imperative to assess the effectiveness of the novel TCI method in TC identification first. In particular, NN, SVM, and RF based identification algorithms, with small scale of inputs from MGD based traffic analysis and 15 inputs selected according to the methods in [31, 32], are tested on 30 combined driving cycles. The 30 driving cycles are also derived based on the traffic data that are collected on real routes [42]. Each driving cycle includes slow-moving, medium-speed drag-free and high-speed transit condition, and partial driving cycles are illustrated in Fig. 6 (a). Tables 4 and 5 list the average classification accuracies and online calculation time from different identification algorithms with two groups of inputs. The numerical results in Tables 6 and 7 highlight the satisfactory performance of the RF based identification algorithm, which can categorize the driving conditions more precisely after using the inputs from the MGD based traffic analysis. Besides, the reduced input scale by MGD based traffic analysis accelerates the online identification speed, boosting the abilities of identification algorithms in real time implementation. Even though the average online calculation time by the RF based identification algorithm is slightly longer than that by SVM, it still can satisfy the requirement of instant application before the vehicle moves into next route segment. To illustrate the behaviours of the proposed novel identification algorithm more clearly, two assessment cases are compared in Fig. 6 (b) and (c). The displayed driving cycles are included in the chosen 30 driving cycles, and the real driving conditions in these cycles are calibrated beforehand. Apparently, the novel identification algorithm based on RF can discern driving conditions precisely in most of time, and the identification errors are mainly incurred by the noise (mainly due to the measurement error and malfunction during data collection) existing in the training data that may induce overfitting and improper categorization. Even with misidentification, most of errors are prone to be sluggishly classified (especially in Fig. 6 (b)); that said, it leads to neglectable impact on the proposed strategy. This is because the threshold optimization in the developed strategy is finalized within a certain segment, exhibiting certain robustness to the lagged classification. Based on the numerical and visual results, it can be concluded that the novel TCI method shows better performance in driving condition classification than the existing methods in literature. The prompted

performance of the novel TCI owes to the MGD based traffic analysis and the enhanced regression by RF. The MGD based analysis can process the connection among state parameters of traffic flow and endow the inputs for identification algorithms with stronger positive correlation. The reduced scale of inputs for identification algorithms boost the capacities of identification algorithms in instant application. To sum up, the RF based identification algorithm possesses qualified capacities in classification problem due to its decision-tree based framework and specific manner to generate output.

Table 6 Numerical comparison in condition identification by different identification algorithms with 15 inputs

Method	Average Accuracy (%)	Average Online Calculation Time (s)
NN	1.219	0.211
SVM	1.136	0.207
RF	0.861	0.209

Table 7 Numerical comparison in condition identification by different identification algorithms with inputs from MGD

Method	Average Accuracy (%)	Average Online Calculation Time (s)
NN	0.949	0.205
SVM	0.893	0.202
RF	0.611	0.204

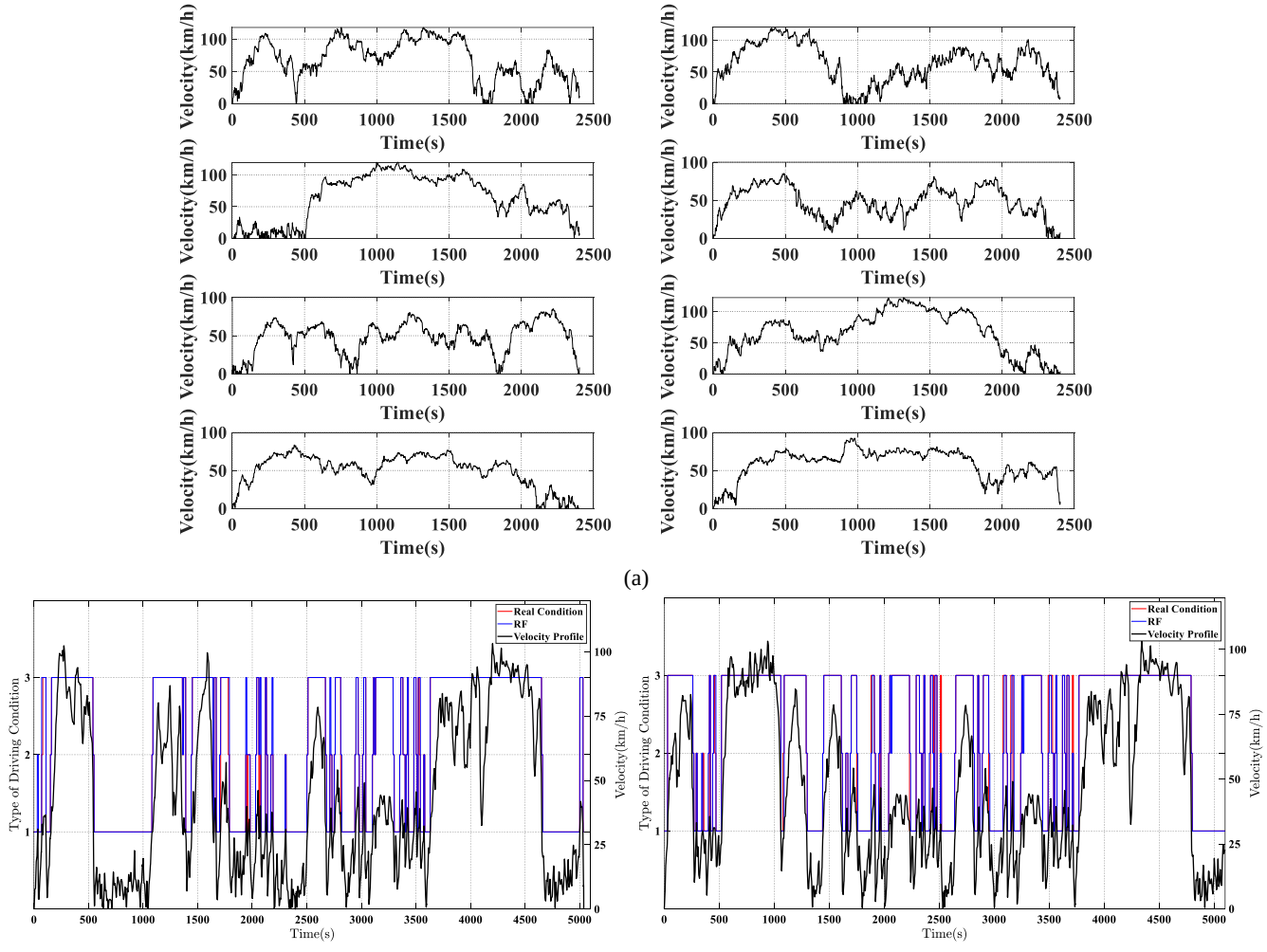

Fig. 6. Illustration of assessment on TCI accuracy. (a) Partial driving cycles in assessment. (b) Condition identification result 1 by NTCI with inputs from MGD based traffic analysis; (c) Condition identification result 2 by NTCI with inputs from MGD based traffic analysis.

B. Study the Role of the Proposed PMS in Energy Saving

After validating the effectiveness of the novel TCI method, the energy saving performance of the raised adaptive PMS needs to be addressed. Under the constraints from the corresponding laws and rules, PHEVs prefer more electricity usage in charging depleting stage based on the designed control thresholds for mode transition and energy distribution. The particular design manner makes it hazy to reveal behaviours of the raised method if the simulation is performed in charging depleting stage in most of time. As such, for better demonstrating the performance of the proposed PMS, the simulation is designed with a low initial battery SOC, i.e., 0.35. Besides, the comparison study in this section only presents the performance of motor 1 since the power distribution ratio between motors 1 and 2 is chosen as 0.5 in this paper. The study on the role of the proposed PMS in energy saving can be divided into three steps. The first step generally investigates the performances of the presented PMS by comparing with some baseline methods in different driving cycles. The second step compares the proposed approach with alternative energy management formulation which implies more complex controller and includes higher level intrinsic adaptability to varying traffic scenarios, further weighing performance of the novel PMS. The third step comparatively analyzes component behaviors of the studied vehicle, elaborately revealing energy-saving mechanism underline the new method.

a. The General Investigation on Performance of the Presented PMS

The general performance of presented PMS is examined based on five driving cycles. The chosen five driving cycles include three standard cycles, i.e., UDDS, US06 and HWFET, as well as two real traffic driving cycles, as shown in Fig. 6 (b) and (c). For ease of evaluating the performance of the presented PMS, the rule based PMS, ECMS and DP are preferred as the baseline methods. Table 8 lists the detailed energy consumption by different methods. The converted fuel consumption includes the equivalent fuel consumption that is converted from electrical energy usage. Intuitively, the presented adaptive PMS leads to better fuel economy, compared with the original rule based PMS and ECMS, and achieves close effect to global DP. The fuel economy of the novel PMS can reach 95.42% of that by DP and can be reduced by as much as 5.91% and 1.23%, compared with that of the rule based PMS and ECMS. The optimality of the novel PMS is better in standard driving cycles than that in real traffic driving cycles. This can be attributed to the following two reasons. First, the accuracy of TCI on standard driving cycles are slightly higher due to the low-frequency TC variation, thus reducing misrecognition especially at the boundaries of neighbouring TCs. Second, the simulation length in standard driving cycles is shorter than that in real traffic driving cycles, resulting in less cumulation error. The comparison between the environmentally sensitive ECMS and novel

PMS proves that the improved adaptability to TCs increases the opportunity to infuse more environment information into power management, thereby furnishing better performance of PMS. The difference in the original CS strategy and novel PMS exhibits that the rule based method can also attain the satisfactory performance by combining optimal knowledge with expert experience.

Table 8 Energy consumption by different methods

Driving Cycle	Strategy	Fuel Consumption (g)	Converted Fuel Consumption (L/100km)	Optimality (%)	Performance Promotion (%)
UDDS	Original CS	398.12	4.35	89.51	-
	ECMS	390.87	4.13	94.19	4.68
	NCS with NTCI	388.12	4.07	95.42	5.91
	DP	376.61	3.89	100	10.49
US06	Original CS	160.01	4.38	89.43	-
	ECMS	157.33	4.15	94.51	5.08
	NCS with NTCI	154.97	4.11	95.29	5.86
	DP	150.34	3.92	100	10.57
HWFET	Original CS	199.06	4.48	89.56	-
	ECMS	194.81	4.25	94.41	4.85
	NCS with NTCI	190.31	4.20	95.32	5.76
	DP	185.13	4.01	100	10.44
Cycle 1	Original CS	1455.41	4.61	89.17	-
	ECMS	1429.02	4.35	94.43	5.26
	NCS with NTCI	1425.33	4.32	95.06	5.89
	DP	1378.51	4.11	100	10.83
Cycle 2	Original CS	1331.68	4.52	89.64	-
	ECMS	1308.79	4.30	94.21	4.57
	NCS with NTCI	1298.16	4.26	95.13	5.49
	DP	1253.16	4.05	100	10.36

b. The Comparison between the Proposed PMS and MPC Based PMS

To further evaluate the power management performance, the novel PMS with TC adaptability is compared with the MPC based PMS under the same simulation conditions. The MPC based PMS searches optimal solutions within predicted horizons and tries to incorporate future TC information into power sources management, thereby holding intrinsic adaptability to varying TCs. Table 9 lists the comparison results between the two PMSs on the real traffic driving cycles shown in Fig. 6 (b) and (c). As can be seen, the fuel consumption by MPC based PMS is slightly lower than that by the novel PMS, while the calculation time by the MPC based PMS is obviously longer. The step calculation time is obtained by dividing the total calculation time over the total number of control steps, and the control step in the study is set to 0.2 s. The better performance of the MPC based PMS in energy saving lies in the benefit from the solution searching in receding horizons. It can find the solution for each step by incorporating the predicted future driving information can fully consider the impact on whole energy consumption in each decision. Whereas, the proposed novel PMS seeks the solution for several steps within a route segment. The rough solution searching scale discounts the performance in energy saving. However, the maximum difference in the converted fuel consumption is merely 0.98%, which can be neglected to some extent. As the implementation of MPC algorithm requests prediction on future driving information, and the complex calculation is burdensome; therefore, the capacity

in real-time application of MPC cannot be as qualified as that of the novel PMS. Considering the balance in fuel economy and application capacity in real time, the performance of the proposed PMS is satisfactory, and it can be treated as an alternative solution to the MPC based PMS.

Table 9 Comparison in MPC and NCS with NTCI

Driving Cycle	Strategy	Converted Fuel Consumption (L/100 km)	Total Calculation Time (s)	Step Calculation Time (s)
Cycle 1	Original CS	4.61	1775.36	0.071
	MPC	4.28	4425.31	0.177
	NCS with NTCI	4.32	2650.06	0.106
Cycle 2	Original CS	4.52	1800.26	0.072
	MPC	4.01	4375.14	0.175
	NCS with NTCI	4.05	2625.21	0.105

c. The Analysis of Energy-Saving Mechanism of the Novel Method

After realizing the satisfying performance of the novel PMS, the energy-saving mechanism of the novel method is further investigated. Fig. 7 (a) and (b) supply the subsidiary illustration on energy consumption manners by different methods. The accumulate fuel consumption shown in Fig. 7 (a) reveals the closed fuel consuming variations between the NCS with NTCI and DP. The approaching fuel consuming way to global DP is realized by incorporating partial driving information into PMS in the raised method through TCI. Specifically, as can be seen, the electric energy is strictly replenished in medium-speed drag-free and high-speed transit condition while utilized in slow-moving condition by DP. The presented method, after integrated with the ability in perceiving the future driving conditions by TCI, can supply the most appropriate control thresholds for future driving, thereby achieving the close effect to global DP. In Fig. 7 (a), the vehicle operates in medium-speed drag-free and high-speed transit condition successively from 1000 s to 1700 s. The NCS with NTCI requires the ICE to charge the battery in serial and parallel mode, respectively, avoiding the similar fast decrease of SOC by the Original CS. The similar manipulation appears in the simulation by DP. The saving electricity can contribute to the vehicle's operation in pure EV mode under slow-moving conditions. Despite the slight difference of SOC by DP, the proposed strategy saves more electric energy for pure EV driving under slow-moving conditions.

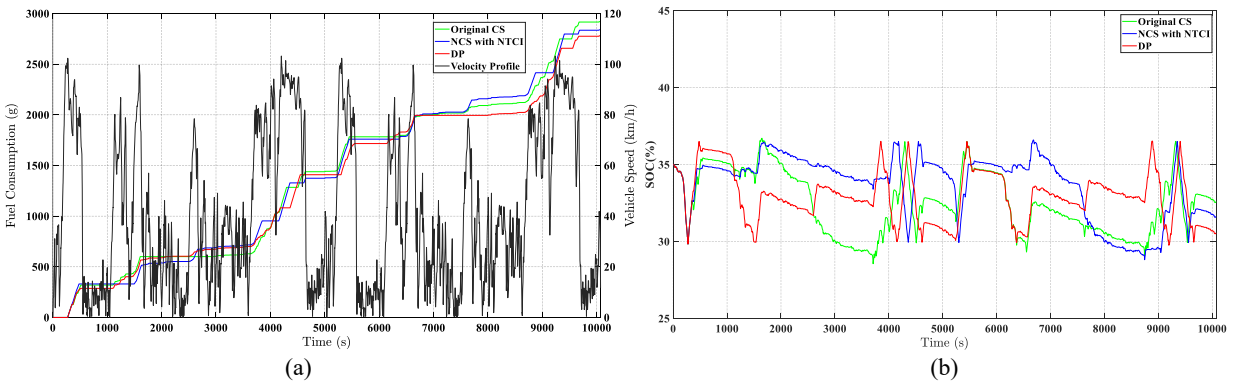

(a) (b)

Fig. 7. Comparison in energy performance. (a) Fuel consumption by different methods; (b) Battery SOC curves by different methods.

Fig. 8 (a) to (c) compare the performance of different methods from the perspective of component operation status. Two cases are marked to demonstrate the behaviours of different methods. In case 1 (from 1700 s to 3000 s), the driving conditions include slow-moving and medium-speed drag-free conditions. The DP and NCS with NTCI endeavour to flatten the SOC decrease rate by enabling the vehicle to operate in serial and parallel mode more. The fast depletion of electricity by Original CS, nevertheless, forces the ICE to operate in both high and low efficiency fields and therefore opposes to energy saving. In case 2, the vehicle operates on high-speed transit condition and slow-moving condition sequentially. The DP and NCS with NTCI take the opportunity to charge the battery in high speed for optimal efficiencies of ICE. Then, in low speed, the replenished electric energy is consumed to avoid the inferior fuel economy operation mode. In contrast, the Original CS requests the ICE to operate in low speed frequently, exaggeratedly increasing the fuel consumption with low efficiency. In reference to the NCS with NTCI, the foreseen traffic condition via NTCI endows the opportunities to adjust control thresholds, adaptively managing energy flow within powertrains effectively.

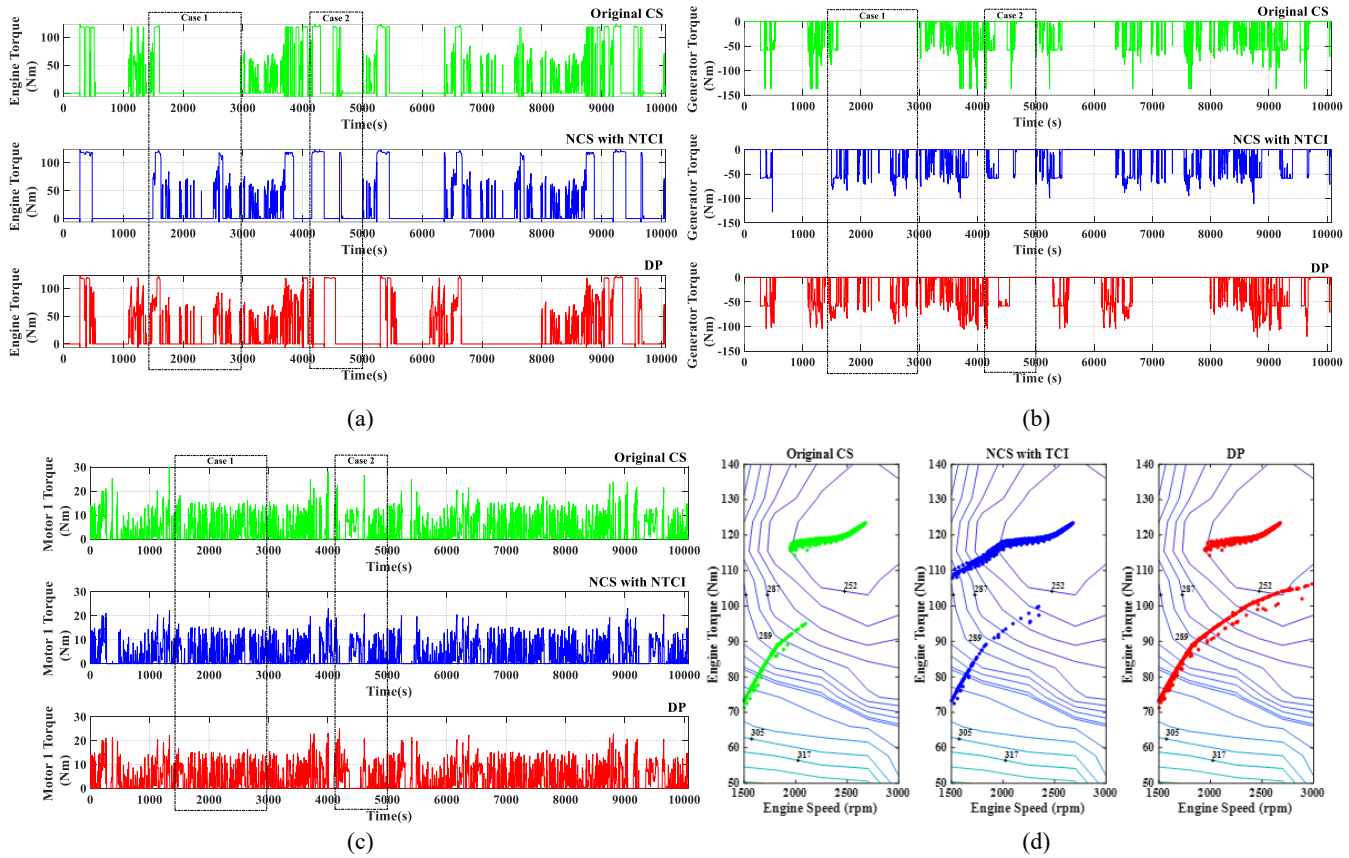

Fig. 8. Comparison in component operation. (a) Comparison in ICE torque by different methods; (b) Comparison in generator torque by different methods; (c) Comparison in motor 1 torque by different methods; (d) Comparison in ICE operation points by different method.

Fig. 8 (d) compares the ICE operation area by different methods. The operation points in high efficiency region by DP and the NCS with NTCI are clearly more than those by Original CS, contributing to better fuel economy. DP, given the knowledge about the whole driving cycle before the trip starts, can search the optimal solution that results

in minimum fuel consumption. While the NCS with NTCI, foreseeing upcoming traffic condition via IoVs, prepares the best control thresholds for next route segment, thereby narrowing the gap to global optimal solution and boosting fuel economy. The enhanced adaptability to varying TCs insures the most appropriate control thresholds can be implemented for current TC, thereby increasing the probabilities that PMS control power sources operate in optimal zones and contributing to fuel economy improvement.

Through the simulation analysis, it can be summarized that the proposed method highlights prompted adaptabilities to various driving conditions by integrating NTCI. Meanwhile, through the cooperation of NTCI, the designed control threshold optimization method superiorly improves the fuel economy of the studied vehicle.

V. CONCLUSION

This paper presents a novel power management strategy for plug-in hybrid electric vehicles with the enhanced adaptability to various traffic conditions. The adaptation to different traffic conditions is realized by the novel traffic condition identification method. According to the identified traffic conditions, the control thresholds are optimized by chaotic particle swarm optimization with sequential quadratic programming offline and updated timely. The main findings can be summarized as follows.

1) The multi-dimension Gaussian distribution based traffic analysis, together with the random forest based classification, improves the accuracy of instant traffic condition categorization.
2) The chaotic particle swarm optimization with sequential quadratic programming refines the ability of simple rule based algorithm, narrowing the gap towards to global optimality.
3) The dramatic adaption to different traffic conditions, together with evolved rule based algorithm, provides the studied plug-in hybrid electric vehicle with the opportunities of advancing its potential in energy saving. Compared with the original rule based strategy, the fuel economy by the raised method is improved by as high as 5.91%, reaching 95.42% of that by the dynamic programming based strategy.
4) The proposed novel power management strategy holds promising capacity in instantly optimal control, which can be seen as an alternative to the model predictive control based management strategy.
5) The improved adaptability to time-varying TCs prompts the application of the polished control thresholds and increases more chances for powertrain components to operate in optimal regions, thereby contributing to fuel economy improvement.

In the future, more efforts will be made in developing new methods to prompt the adaptability of power management strategies to traffic conditions. In addition, novel methods such as machine learning will be employed

to improve the traffic condition precision. Furthermore, impact on vehicle performance in real time from driving behaviours will also be carefully investigated.

ACKNOWLEDGEMENT

This work was supported in part by the National Natural Science Foundation of China (No. 61763021 and No. 51775063), in part by the National Key R&D Program of China (No. 2018YFB0104900), and in part by the EU-funded Marie Skłodowska-Curie Individual Fellowships under Grant 845102-HOEMEV-H2020-MSCA-IF-2018.

REFERENCE

[1] Y. Zhang, et al. , "Energy management strategy for plug-in hybrid electric vehicle integrated with vehicle-environment cooperation control," *Energy (2020)* p. 117192.

[2] X. Hu, et al., "Model predictive control of hybrid electric vehicles for fuel economy, emission reductions, and inter-vehicle safety in car-following scenarios.," *Energy 196 (2020),* p. 117101.

[3] Shan, Zhenyu, et al. "Synthesis of Multi-Input Multi-Output DC/DC Converters Without Energy Buffer Stages." *IEEE Transactions on Circuits and Systems II: Express Briefs* (2020).

[4] Zhou, Wei, et al. "Dynamic programming for New Energy Vehicles based on their work modes part I: Electric Vehicles and Hybrid Electric Vehicles." *Journal of Power Sources* 406 (2018): 151-166.

[5] Du, Ronghua, et al. "Battery aging-and temperature-aware predictive energy management for hybrid electric vehicles." Journal of Power Sources 473 (2020): 228568.

[6] Zhou, Yang, et al. "An integrated predictive energy management for light-duty range-extended plug-in fuel cell electric vehicle." Journal of Power Sources 451 (2020): 227780.

[7] B. V. Padmarajan, Andrew McGordon, and Paul A. Jennings., " Blended rule-based energy management for PHEV: System structure and strategy.," *IEEE Transactions on Vehicular Technology 65.10 (2015),* pp. 8757-8762.

[8] Gao, Dawei, Zhenhua Jin, and Qingchun Lu. "Energy management strategy based on fuzzy logic for a fuel cell hybrid bus." Journal of Power Sources 185.1 (2008): 311-317.

[9] Zhou, Wei, et al. "Dynamic programming for new energy vehicles based on their work modes Part II: Fuel cell electric vehicles." Journal of Power Sources 407 (2018): 92-104.

[10] S. Xie, et al. , "Pontryagin's minimum principle based model predictive control of energy management for a plug-in hybrid electric bus.," *Applied energy 236 (2019),* pp. 893-905.

[11] X. Tian, et al. , "An adaptive ECMS with driving style recognition for energy optimization of parallel hybrid electric buses.," *Energy 189 (2019),* p. 116151.

[12] J. Li, et al. , "Research on Equivalent Factor Boundary of Equivalent Consumption Minimization Strategy for PHEVs.," *IEEE Transactions on Vehicular Technology (2020).*

[13] Sun, Haochen, et al. "Data-driven reinforcement-learning-based hierarchical energy management strategy for fuel cell/battery/ultracapacitor hybrid electric vehicles." Journal of Power Sources 455 (2020): 227964.

[14] Y. Wu, et al. , "Deep reinforcement learning of energy management with continuous control strategy and traffic information for a series-parallel plug-in hybrid electric bus.," *Applied Energy 247 (2019),* pp. 454-466.

[15] S. G. Wirasingha, and Ali Emadi. , "Classification and review of control strategies for plug-in hybrid electric vehicles.," *IEEE Transactions on vehicular technology 60.1 (2010),* pp. 111-122.

[16] H. Tian, et al., "Adaptive fuzzy logic energy management strategy based on reasonable SOC reference curve for online control of plug-in hybrid electric city bus.," *IEEE Transactions on Intelligent Transportation Systems 19.5 (2017),* pp. 1607-1617.

[17] S. Moura, "HW 5: Optimal PHEV Energy Management via Dynamic Programming.," *University of California, Berkeley(2018).*

[18] W. Lee, et al. , "An Adaptive Concept of PMP-Based Control for Saving Operating Costs of Extended-Range Electric Vehicles.," *IEEE Transactions on Vehicular Technology68.12 (2019),* pp. 11505-11512.

[19] Y. Yang, et al., "Adaptive real-time optimal energy management strategy for extender range electric vehicle.," *Energy (2020),* p. 117192.

[20] Z. Lei, et al., "An adaptive equivalent consumption minimization strategy for plug-in hybrid electric vehicles based on traffic information.," *Energy 190 (2020),* p. 116409.

[21] Y. Zhang, et al., "An improved adaptive equivalent consumption minimization strategy for parallel plug-in hybrid electric vehicle.," *Proceedings of the Institution of Mechanical Engineers, Part D: Journal of Automobile Engineering 233.6 (2019),* pp. 1649-1663.

[22] C. Yang, et al. , "A stochastic predictive energy management strategy for plug-in hybrid electric vehicles based on fast rolling optimization.," *IEEE Transactions on Industrial Electronics (2019).*

[23] K. Song, et al. , "Multi-mode energy management strategy for fuel cell electric vehicles based on driving pattern identification using learning vector quantization neural network algorithm.," *Journal of Power Sources 389 (2018),* pp. 230-239.

[24] Y. U. Rong, et al. , "Urban road traffic condition pattern recognition based on support vector machine.," *Journal of Transportation Systems Engineering and Information Technology 13.1 (2013),* pp. 130-136.
[25] C. Sun, et al., "Velocity predictors for predictive energy management in hybrid electric vehicles.," *IEEE Transactions on Control Systems Technology 23.3 (2014),* pp. 1197-1204.
[26] J. Shin, and Myoungho Sunwoo., "Vehicle speed prediction using a Markov chain with speed constraints.," *IEEE Transactions on Intelligent Transportation Systems 20.9 (2018),* pp. 3201-3211.
[27] M. Dabbaghjamanesh, Amirhossein Moeini, and Abdollah Kavousi-Fard. , "Reinforcement Learning-based Load Forecasting of Electric Vehicle Charging Station Using Q-LearningTechnique.," *IEEE Transactions on Industrial Informatics (2020).*
[28] C. Song, et al., "A power management strategy for parallel PHEV using deep Q-Networks.," *2018 IEEE Vehicle Power and Propulsion Conference (VPPC). IEEE, 2018.*
[29] Z.-k. Feng, et al., "Operation rule derivation of hydropower reservoir by k-means clustering method and extreme learning machine based on particle swarm optimization.," *Journal of Hydrology 576 (2019),* pp. 229-238.
[30] X. Gao, L. Dai , and A. M. Sayeed . , "Low RF-Complexity Technologies to Enable Millimeter-Wave MIMO with Large Antenna Array for 5G Wireless Communications.," *IEEE Communications Magazine(2016),* pp. 2-8.
[31] L. Shuxian, et al., "Energy Management Strategy for Hybrid Electric Vehicle Based on Driving Condition Identification Using KGA-Means.," *Energies 11.6(2018),* p. 1531.
[32] S. Ishak, and Ciprian Alecsandru. , "Optimizing traffic prediction performance of neural networks under various topological, input, and traffic condition settings.," *Journal of Transportation Engineering 130.4 (2004),* pp. 452-465.
[33] A. Hantoute, René Henrion, and Pedro Pérez-Aros. , "Subdifferential characterization of probability functions under Gaussian distribution.," *Mathematical Programming 174.1-2 (2019),* pp. 167-194.
[34] M. Belgiu, and Lucian Drăguț. , "Random forest in remote sensing: A review of applications and future directions.," *ISPRS Journal of Photogrammetry and Remote Sensing 114 (2016),* pp. 24-31.
[35] G. Biau, and Erwan Scornet. , "A random forest guided tour.," *Test 25.2 (2016),* pp. 197-227.
[36] Y. Ding, et al. , "The accuracy and efficiency of GA and PSO optimization schemes on estimating reaction kinetic parameters of biomass pyrolysis.," *Energy 176 (2019),* pp. 582-588.
[37] C. Ju, et al. , "A PSO based energy efficient coverage control algorithm for wireless sensor networks.," *Computers, Materials & Continua 56.3 (2018),* pp. 433-446.
[38] T. A. A. Victoire, and A. Ebenezer Jeyakumar. , "Hybrid PSO–SQP for economic dispatch with valve-point effect.," *Electric Power Systems Research 71.1 (2004),* pp. 51-59.
[39] P. E. Gill, Walter Murray, and Michael A. Saunders., "SNOPT: An SQP algorithm for large-scale constrained optimization.," *SIAM review 47.1 (2005),* pp. 99-131.
[40] Z. Liu, Fahim Forouzanfar, and Yu Zhao. , "Comparison of SQP and AL algorithms for deterministic constrained production optimization of hydrocarbon reservoirs.," *Journal of Petroleum Science and Engineering 171 (2018),* pp. 542-557.
[41] W. Gao, and Donald Goldfarb., "Quasi-Newton methods: superlinear convergence without line searches for self-concordant functions.," *Optimization Methods and Software34.1 (2019),* pp. 194-217.
[42] H. Hongwen, et al. , "Real-time global driving cycle construction and the application to economy driving pro system in plug-in hybrid electric vehicles.," *Energy 152 (2018),* pp. 95-107.